PTEP

Prog. Theor. Exp. Phys. **2016**, 043D03 (12 pages)
DOI: 10.1093/ptep/ptw027

Quadrupole and monopole transition properties of 0_2^+ in Gd isotopes

Masayuki Matsuzaki* and Tomoya Ueno

Department of Physics, Fukuoka University of Education, Munakata, Fukuoka 811-4192, Japan
*E-mail: matsuza@fukuoka-edu.ac.jp

Received January 4, 2016; Revised February 10, 2016; Accepted February 22, 2016; Published April 15, 2016

The longstanding problem of characterization of the 0_2^+ states in Gd isotopes is revisited by adopting the Nilsson+BCS mean field and the random-phase approximation. The interband electric quadrupole transition strengths varying almost two orders of magnitude are nicely reproduced at the same time as other observables. These results indicate that the 0_2^+ states, in particular those in lighter isotopes, are well described as β vibrations excited on top of deformed ground states without recourse to the shape-coexistence picture.

Subject Index D12, D13

1. Introduction

The first 0^+ excitation, denoted as 0_2^+, is one of the fundamental excitations in atomic nuclei. It carries information about the nuclear shape and the pairing correlation. In medium and heavy nuclei, ground states of those which are off closed shell are more or less deformed. In the traditional picture of Bohr and Mottelson, their deformations are axially symmetric and the β $\left(K^\pi = 0^+\right)$ and γ $\left(K^\pi = 2^+\right)$ vibrations exist as low-lying collective excitations [1]. Actually, the latter has been widely confirmed in the nuclear chart. In contrast, properties of observed 0_2^+ are still controversial [2]. The most decisive observable is $B\left(E2, 0_2^+ \to 2_1^+\right)$, but its data often have relatively large error bars and they vary strongly with nucleon numbers.

Not only as a particle–hole collective state, the shape vibration, but 0^+ states can be excited as a particle–particle collective state, pairing vibration, via two-nucleon (2n) transfer reactions. In superfluid nuclei, their typical cross-section to 0_2^+ is estimated as 2% of that to 0_1^+ [3]. In the 1970s, a lot of (p, t) and (t, p) experiments were done and it was found that transfer cross-sections to 0_2^+ became comparable with those to 0_1^+ in transitional $N = 88$–90 nuclei; see Ref. [4] for the example of Gd. Their results were interpreted mainly in terms of the shape-coexistence picture [5,6], for example. On the other hand, a large-amplitude shape fluctuation encompassing two minima, if existent, was also conjectured [7].

Another observable that is known to be sensitive to shape deformation and coexistence is $\rho^2(E0)$, the reduced electric monopole transition strength measured through internal electron conversions [8,9]. The latter reference discussed a wide variety of medium and heavy nuclei based on available data of $0^+ \to 0^+$, $2^+ \to 2^+$, and $4^+ \to 4^+$ transitions. On the other hand, the $E0$ transition strength is one of the indicators of the cluster structure in light nuclei [10]. Reference [11] compiles

$0^+ \to 0^+$ transition data throughout the nuclear chart. Theoretically, the $E0$ strengths in medium-heavy nuclei have been systematically studied mainly in terms of the interacting boson approximation (IBA) model [12], for example. But characterization of 0_2^+ is still not decisive. This suggests that not only properties of 0_2^+, such as the level energy and $E2$ and $E0$ transitions to the ground band, but also other information such as rotational band structure should be taken into account. Studies aiming at such a direction were pursued for ^{152}Sm, for example [13–15]. In addition, the relation between the properties of the 0_2^+ in ^{154}Gd and the spectra of an adjacent odd-A nucleus was also argued, trying to discriminate different pictures [16,17].

In the following, we study $B\left(E2, 0_2^+ \to 2_1^+\right)$, $\rho^2\left(E0, 0_2^+ \to 0_1^+\right)$, and their ratio, $X(E0/E2)$, of Gd isotopes that is one of the isotope chains about which the richest information is available, paying attention also to rotational properties. Experimental data are taken from the Live Nuclear Chart of the IAEA [18] for level energies and $B(E2)$, and from Ref. [11] for $\rho^2(E0)$.

2. The model

We adopt a traditional mean field + random-phase approximation (RPA). The mean field is the Nilsson + BCS model,

$$h = h_{\rm Nil} - \Delta_\tau \left(P_\tau^\dagger + P_\tau\right) - \lambda_\tau N_\tau, \quad \tau \in \{n, p\},$$

$$h_{\rm Nil} = \frac{\mathbf{p}^2}{2M} + \frac{1}{2}M\left(\omega_x^2 x^2 + \omega_y^2 y^2 + \omega_z^2 z^2\right) + v_{ls}\mathbf{l}\cdot\mathbf{s} + v_{ll}\left(\mathbf{l}^2 - \left\langle \mathbf{l}^2\right\rangle_{N_{\rm osc}}\right),$$

where standard notations for each quantity are understood. The $\mathbf{l}\cdot\mathbf{s}$ and $\mathbf{l}^2$ terms are given by the singly stretched coordinates. Their strengths are taken from Ref. [19]. The deformation of the oscillator potential is parameterized as

$$\omega_j = \omega_0\left[1 - \frac{2}{3}\epsilon_2 \cos\left(\gamma + \frac{2\pi\nu_j}{3}\right)\right], \quad j \in \{x, y, z\},$$

$$\nu_x = 1, \quad \nu_y = -1, \quad \nu_z = 0,$$

where ω_0 is determined so as to conserve the nuclear volume. The cranking term $-\hbar\omega_{\rm rot}J_x$ is also introduced when necessary. The residual pairing (P) plus isoscalar doubly stretched quadrupole–quadrupole (Q–Q) interaction is given by

$$H_{\rm int} = -G_\tau \widetilde{P_\tau}^\dagger \widetilde{P_\tau} - \frac{1}{2}\sum_{K=0}^{2} \kappa_K^{(+)} \widetilde{Q_K''^{(+)}}^\dagger \widetilde{Q_K''^{(+)}},$$

where $Q_K''^{(+)}$ are obtained from the spherical harmonics as

$$Q_{2\mu}(\mathbf{r}) = r^2 Y_{2\mu}(\theta, \phi),$$

$$Q_K^{(+)}(\mathbf{r}) = \frac{1}{\sqrt{2(1+\delta_{K0})}}\left(Q_{2K}(\mathbf{r}) + Q_{2-K}(\mathbf{r})\right),$$

$$Q_K''^{(+)} = Q_K^{(+)}\left(x_j \to x_j'' = \frac{\omega_j}{\omega_0}x_j\right).$$

Here, "$\sim$" indicates that the ground-state expectation values are subtracted, and the $K \neq 0$ terms mix into the mode under consideration when a rotation and/or γ deformation are introduced. The original P+Q–Q interaction was used to determine the parameters of Bohr's collective Hamiltonian [20] and applied to deformed Gd isotopes in Ref. [21]. The doubly stretched Q–Q interaction was proposed

to fulfill a shape self-consistency in deformed nuclei and was shown to be effective in the actual description of deformed nuclei [22,23], and further extended to rotating nuclei [24].

Transition strengths are calculated as follows. For the initial state $|\mathrm{i}\rangle = \left|0_2^+\right\rangle = X^\dagger\left|0_1^+\right\rangle$ and the final state $|\mathrm{f}\rangle = \left|2_1^+\right\rangle$, where 2_1^+ is the first excited member of the ground-state band, the $E2$ transition strength is given by

$$B\left(E2, I_\mathrm{i}K_\mathrm{i} = 0 \to I_\mathrm{f}K_\mathrm{f} = 0\right) = \left\langle I_\mathrm{i}020|I_\mathrm{f}0\right\rangle^2 \left|\left\langle\left[Q_0^{(+)}, X^\dagger\right]\right\rangle_\mathrm{RPA}\right|^2,$$

when the rotational effect, the difference between the intrinsic states of $\left|0_1^+\right\rangle$ and $\left|2_1^+\right\rangle$, is ignored. Here, $\left\langle I_\mathrm{i}020|I_\mathrm{f}0\right\rangle = 1$ for $I_\mathrm{i} = 0$, $I_\mathrm{f} = 2$, and $\left\langle\left[\cdot, X^\dagger\right]\right\rangle_\mathrm{RPA}$ denotes the transition amplitude associated with the RPA phonon $X^\dagger$. The rotational effect is taken into account by the method [25] based on the generalized intensity relation (GIR) [1]. The GIR indicates that the angular momentum dependence of interband transition matrix elements fits into the form $M_1 + M_2\left[I_\mathrm{f}\left(I_\mathrm{f}+1\right) - I_\mathrm{i}\left(I_\mathrm{i}+1\right)\right]$. In the textbook of Bohr and Mottelson, M_1 and M_2 are obtained by fitting to the data. Such a fit was also done for adjacent nuclei recently [15]. Reference [25] proposed a method to represent it in terms of intrinsic matrix elements given by the mean field and RPA. The concrete form for the present case is given by replacing

$$\begin{aligned}
&M_1 = \left\langle\left[Q_0^{(+)}, X^\dagger\right]\right\rangle_\mathrm{RPA} \to \\
&M_1 + M_2\left[I_\mathrm{f}\left(I_\mathrm{f}+1\right) - I_\mathrm{i}\left(I_\mathrm{i}+1\right)\right] \\
&\quad = \left\langle\left[Q_0^{(+)}, X^\dagger\right]\right\rangle_\mathrm{RPA} + \frac{\hbar}{2\sqrt{3}\mathcal{J}}\frac{\mathrm{d}}{\mathrm{d}\omega_\mathrm{rot}}\left\langle\left[Q_1^{(+)}, X^\dagger\right]\right\rangle_\mathrm{RPA}\left[I_\mathrm{f}\left(I_\mathrm{f}+1\right) - I_\mathrm{i}\left(I_\mathrm{i}+1\right)\right],
\end{aligned}$$

where $\mathcal{J}$ is the moment of inertia of the ground-state band.

The non-dimensionalized $E0$ transition matrix element from $|\mathrm{i}\rangle = \left|0_2^+\right\rangle = X^\dagger\left|0_1^+\right\rangle$ to $|\mathrm{f}\rangle = \left|0_1^+\right\rangle$ is given by

$$\rho\left(E0, \mathrm{i} \to \mathrm{f}\right) = \left\langle\left[r^2, X^\dagger\right]\right\rangle_\mathrm{RPA} \Big/ eR^2,$$

with $R = r_0A^{1/3}$. Effective charges are not introduced, and $Q_K^{(+)}$ and r^2 in these expressions are understood as their proton part multiplied by e. The X ratio [8] is defined by

$$X\left(E0/E2\right) = \frac{\left(\rho\left(E0\right)\right)^2 e^2R^4}{B\left(E2\right)}.$$

3. Results and discussion

3.1. *The shape of ground states*

First of all, quadrupole deformations of the ground states of $^{146\text{–}160}_{82\text{–}96}$Gd are determined by using the Nilsson–BCS–Strutinsky method [26] assuming $\epsilon_4 = 0$, where ϵ_4 is the magnitude of the hexadecapole deformation of the mean field. Calculations were done adopting five major shells $N_\mathrm{osc} = 4$–8 for neutrons and $N_\mathrm{osc} = 3$–7 for protons. The obtained ϵ_2 are summarized in Table 1. For all the cases, $\gamma = 0$.

The lightest two, ^{146}Gd and ^{148}Gd, are spherical, $\epsilon_2 = 0$, as expected and they are omitted in Table 1 and the following calculation. The next one, ^{150}Gd, is almost spherical, $\epsilon_2 = 0.07$. Experimentally the two-phonon triplet in terms of spectra of spherical nuclei splits to some extent and the 0^+ among them was labeled as the quasi-β [27]. A boson expansion calculation included in that reference shows a more developed rotational character. Then we included ^{150}Gd in the following figures for the sake of comparison but obviously the N dependence is discontinuous to ^{152}Gd and heavier.

Table 1. The deformation of the ground state determined by the Nilsson–BCS–Strutinsky method and the experimental data used to determine the properties of Gd isotopes. Among them, the pairing gaps are obtained by the third difference of the experimental masses.

N	ϵ_2	Δ_n (MeV)	Δ_p (MeV)	$E_{0_2^+}$ (MeV)	$E_{2_\gamma^+}$ (MeV)	$E_{2_1^+}$ (MeV)
86	0.07	1.00	1.42	1.207	1.430	0.638
88	0.18	1.11	1.48	0.615	1.109	0.344
90	0.22	1.28	1.13	0.681	0.996	0.123
92	0.25	1.07	0.96	1.049	1.154	0.089
94	0.27	0.89	0.88	1.196	1.187	0.080
96	0.26	0.83	0.85	1.380	0.988	0.075

In the literature, the ground state of ^{152}Gd has been said to be spherical and this led to the shape-coexistence interpretation of the $2n$-transfer data [4], but the present result of the Strutinsky method disagrees. In the following we put some emphasis on this issue.

3.2. *Transition strengths*

3.2.1. *N dependence*

Adopting the deformation ϵ_2 obtained above, the mean field plus RPA calculations are performed in three major shells $N_{\rm osc} = 4$–6 for neutrons and $N_{\rm osc} = 3$–5 for protons, which give phenomenologically appropriate results, as in Ref. [25]. Interaction strengths G_n, G_p, and $\kappa_K^{(+)}$ ($K = 0, 2$) are adjusted to reproduce experimental pairing gaps, $E_{0_2^+}$ and $E_{2_\gamma^+}$ tabulated in Table 1. The $K = 1$ component is adjusted to give zero energy to the Nambu–Goldstone mode.

Figure 1(a) presents the most important quantity to characterize 0_2^+, $B(E2)$ to the ground band. The results of calculations with and without inclusion of the rotational effect are compared with the data. They vary by almost two orders of magnitude. This steep variation is nicely reproduced by including the rotational effect. Its significance is shown in Fig. 1(b) by the ratio M_2/M_1. The effect is conspicuous in lighter isotopes because of its dependence on $\mathcal{J}$ determined from $E_{2_1^+} = 2 \cdot (2+1)\hbar^2/2\mathcal{J}$ in Table 1. This is in great contrast to the γ vibration for which the corresponding $\frac{5}{2} \times B\left(E2, 2_\gamma^+ \to 0_1^+\right)$ stays within 10–20 W.u. [Fig. 5(b)]. From this largeness of $B\left(E2, 0_2^+ \to 2_1^+\right)$, the 0_2^+ states in ^{152}Gd and ^{154}Gd have been thought of as typical β vibrations [2,13,28], but a different interpretation was also proposed, as discussed later. The smallness in heavier isotopes, already presented in Ref. [25], will also be discussed later.

Figure 2 compares the result for $\rho^2\left(E0, 0_2^+ \to 0_1^+\right)$ with the available data [11]. Note that Refs. [29,30] included a data point of $\rho^2\left(E0, 0_2^+ \to 0_1^+\right)$ in their calculation for ^{158}Gd, but this is actually that of $\rho^2\left(E0, 2_2^+ \to 2_1^+\right)$—see Refs. [9,31]. A recent large-scale calculation adopting the constrained Hartree–Fock–Bogoliubov theory with the Gogny D1S interaction [32] results in failure to reproduce the order of magnitudes of the observed $\rho^2(E0)$. Then we have to have recourse to more phenomenological models to discuss their actual isotope dependence. In the literature, the IBA model [33] and the geometrical coherent-state model [34] reproduce the data well. The present calculation gives similar results.

The next aspect is the isotope dependence. Preceding the data for $N = 92$, Ref. [12] argued that the rise from $N = 88$ to 90 as well as in other isotope chains is a signal of the spherical-deformed shape phase transition and consequently $\rho^2(E0)$ would stay large in heavier isotopes. Unfortunately this has not been proved to apply. In the present calculation, the maximum occurs at $N = 88$ not 90.

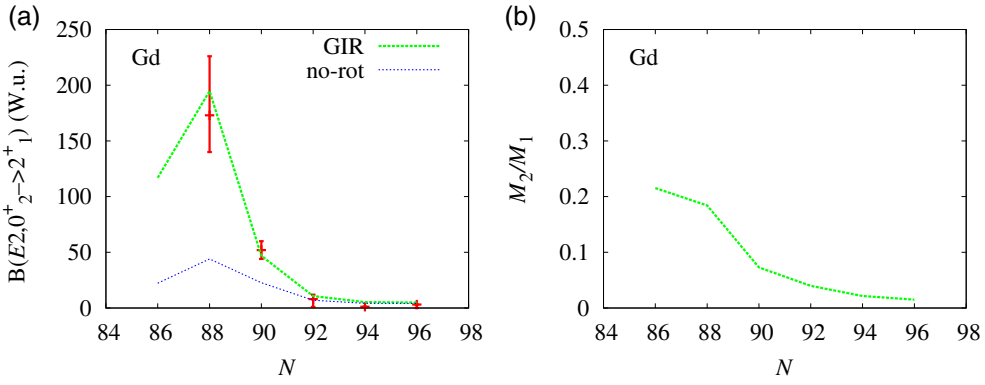

Fig. 1. (a) Experimental and calculated $B\left(E2, 0_2^+ \to 2_1^+\right)$ in the Weisskopf unit as functions of the neutron number of Gd isotopes. Green dashed and blue dotted curves represent the calculations with and without the rotational effect given by the method based on the GIR. Data are taken from Ref. [18]. (b) The ratio M_2/M_1 that gives the magnitude of the rotational effect on the transition matrix element.

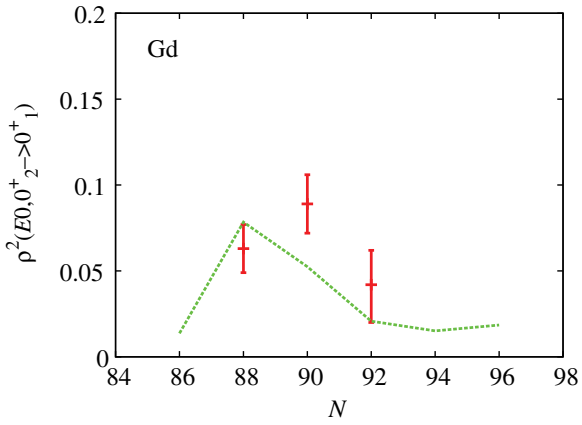

Fig. 2. Experimental and calculated $\rho^2\left(E0, 0_2^+ \to 0_1^+\right)$ as functions of the neutron number of Gd isotopes. The rotational effect does not appear in this quantity. Data are taken from Ref. [11].

Figure 3 compares the calculated X ratios to the data. The reason why Refs. [35,36] included a data point of ^{158}Gd is the same as above. This figure indicates that the isotope dependence is predominantly determined by the denominator. The present calculation reproduces the rising trend but it is quantitatively weaker. This comes from the result that $B(E2)$ in heavier isotopes looks to be larger than the data. This point will be discussed later. The discontinuity between $N = 86$ and 88 seen in Figs. 1(a) and 2 disappears because both the denominator and numerator vary to a similar extent.

3.2.2. Individual nucleus

(1) ^{152}*Gd.* In the literature, ground states of $N = 88$ isotones have been considered to be spherical; see, for example, Refs. [7] for Sm and [4] for Gd. However, the observed in-band $B\left(E2, 2_1^+ \to 0_1^+\right) = 73^{+7}_{-6}$ W.u. [18] suggests a moderate deformation, and actually in the present calculation, the rotational-model expression gives

$$B\left(E2, 2_1^+ \to 0_1^+\right) = \left(eQ_0\right)^2 = 75\,\text{W.u.}$$

In this nucleus, high-spin states of the 0_1^+ and 0_2^+ bands were studied in the 2000s [37,38]. These works show smooth behavior of these bands starting from the bandhead with gradual stretching.

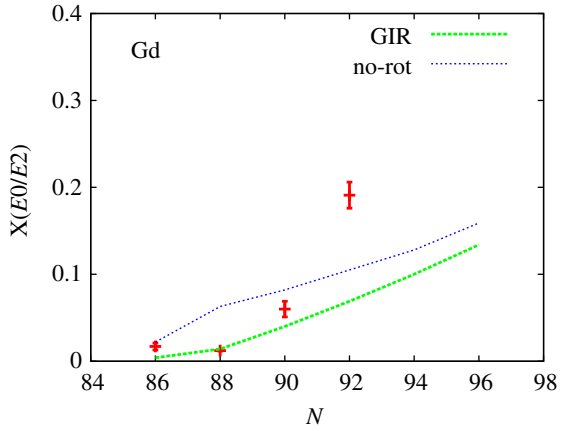

Fig. 3. Experimental and calculated non-dimensionalized ratio of $E0$ and $E2$ transition strengths graphed in the same manner as Fig. 1(a). Data are taken from Ref. [11].

Moreover, a g factor measurement of 2_1^+–6_1^+ also supports the rotational character of the low-spin members of the ground-state band [39]. Actually, the present calculation gives a smooth behavior as a function of the rotational frequency, for example, $g = \frac{\langle \mu_x \rangle}{\langle J_x \rangle} = 0.41$ at $\hbar\omega_{\rm rot} = \frac{E_{2_1^+}}{2} = 0.172\,{\rm MeV}$, which is very close to the collective value, $g_{\rm R} = \frac{Z}{A}$.

Next, an implication of the conspicuous magnitude of $B\left(E2, 0_2^+ \to 2_1^+\right)$ is mentioned. As first discussed by Kumar [40], not only in-band but also interband $B(E2)$ brings information about the deformation. Based on this, the model-independent effective deformation, $\beta_{\rm eff}$, is examined and compared with the IBA model [41]. According to this work, the square of the effective deformation of the 0_2^+ state is given by

$$|\beta_{\rm eff}|^2 = \frac{\sum_j B\left(E2, 0_2^+ \to 2_j^+\right)}{\left(\frac{3}{4\pi} ZeR^2\right)^2}.$$

The summation is expected to be almost saturated with $j = 1$ and 2. In the present mean field plus RPA model, the $j = 2$ term gives the static deformation of the 0_2^+ state while the $j = 1$ term gives the zero-point amplitude of the β vibration. Those converted by

$$\beta_0 = \frac{\sqrt{B\left(E2, 0_2^+ \to 2_1^+\right)}}{\frac{3}{4\pi} ZeR^2}$$

from the $B(E2)$ values in Fig. 1(a) are compared with the corresponding static deformation,

$$\beta_{\rm s} = \frac{\langle Q_0 \rangle_{\rm IS}}{\frac{3}{4\pi} AR^2},$$

in Fig. 4. Here, the subscript designates the isoscalar quadrupole moment.

The RPA is a small-amplitude approximation. It is not obvious from the ratio of $\beta_0 = 0.073$ (no-rot) to $\beta_{\rm s} = 0.207$ whether ^{152}Gd is situated within the applicability of the RPA. In order to look into this, we compare the interband/in-band ratio of $B(E2)$ to the case of the wobbling that is another example of strong interband $E2$ transitions previously accounted for in terms of the RPA. In the present case,

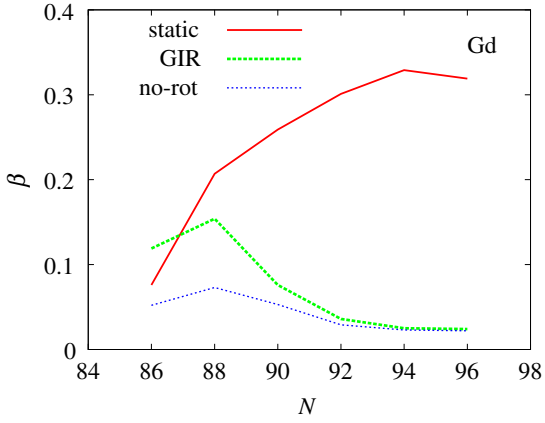

Fig. 4. Calculated static deformation β_s (red solid line) and zero-point amplitudes β_0 of the β vibration with (green dashed line) and without (blue dotted line) the rotational effect as functions of the neutron number of Gd isotopes.

the calculated ratio of the $j = 1$ (interband) and $j = 2$ (in-band) terms,

$$\frac{B\left(E2, 0_2^+ \to 2_1^+\right)}{B\left(E2, 0_2^+ \to 2_2^+\right)} = \frac{B\left(E2, 0_2^+ \to 2_1^+\right)}{B\left(E2, 0_1^+ \to 2_1^+\right)} = \frac{B\left(E2, 0_2^+ \to 2_1^+\right)}{5 \times B\left(E2, 2_1^+ \to 0_1^+\right)},$$

amounts to 0.12 (no-rot) and 0.52 (GIR). The wobbling excitations in the triaxially super/strongly deformed states in Lu isotopes were observed [42–44] and calculated in terms of the RPA [45–49] and in other models [50–52]. Their ratios are $\frac{B\left(E2, I \to I-1\right)}{B\left(E2, I \to I-2\right)} \sim 0.2$. The associated fluctuation, the wobbling angle θ, is about 0.44 radians, for example, which fulfills a criterion of validity of the small amplitude approximation, $\tan\theta \simeq \theta$ [48]. In comparison of the present ratio, 0.12 that is directly given by the RPA, with that of the wobbling case, 0.2, we consider that the RPA is applicable to the β vibration in ^{152}Gd. Then, the effective value, $\beta_0 = 0.154$ (GIR), looks to indicate that, even if there exists some difference between the equilibrium deformations of 0_1^+ and 0_2^+ that is ignored in the present model, it would be of little relevance, as conjectured in Ref. [7].

This strong interband transition is an outcome of strong ground-state correlations, in other words, large backward amplitudes. These backward amplitudes stem from time-reversal pairs near the Fermi surface, such as $|\phi| = 0.916$, 0.959, and 0.699 for $\left(\nu[532]\frac{3}{2}\right)^2$, $\left(\nu[530]\frac{1}{2}\right)^2$, and $\left(\nu[521]\frac{3}{2}\right)^2$, respectively, in the present case, as discussed in the case of ^{154}Gd below. Consequently, the pair transfer cross-section is also expected to be enhanced without recourse to the shape coexistence. Actually, it is shown in Ref. [53] that the ^{154}Gd (p, t) ^{152}Gd cross-section is stronger for 0_2^+ than for 0_1^+. This fact does not contradict the RPA result.

(2) ^{154}*Gd.* The 0_2^+ state at $E = 681$ keV in this nucleus is another candidate of typical β vibrations [2]. In contrast, the 0_3^+ state at $E = 1182$ keV is thought to have a smaller deformation [54] and to be a pairing isomer [28,55]. Higher-lying states above 1 MeV were also investigated [56]. Although a possibility of interpreting the 2^+ state at $E = 1531$ keV as the $\beta \otimes \gamma$ double excitation assuming that the 0_2^+ is a β vibration is reserved, the authors of this reference suggest that the 0_2^+ state has a shape different from that of the ground state rather than is the β vibration on top of it based on the non-existence of the two-phonon β vibrational state. A similar argument was also presented

Table 2. The results of the RPA calculation for each configuration. Among them, $\Delta_{\rm n}$ and $\hbar\omega_\beta = E_{0_2^+}$ of ^{154}Gd are fitted to the data (Table 1). $\sum\phi^2$ denotes the sum of the squared backward amplitudes in the RPA phonon. $t^2_{Q_0^{(+)}}$ is equal to $B\left(E2, 0_2^+ \to 2_1^+\right)$ without the rotational effect in the case of the even–even nucleus.

nucleus	band	$\Delta_{\rm n}$ (MeV)	$\hbar\omega_\beta$ (MeV)	$\sum\phi^2$	$t^2_{Q_0^{(+)}}$ (W.u.)
^{154}Gd	ground	1.28	0.681	3.07	22.7
^{155}Gd	$[521]\frac{3}{2}$	1.10	0.974	1.39	13.6
^{155}Gd	$[505]\frac{11}{2}$	1.16	1.475	0.47	8.9

for ^{152}Sm [57,58], but the non-existence of the two-phonon β vibrational state does not necessarily mean that of the one phonon.

Reference [16] further proceeds in this direction; the 0_2^+ is also a pairing isomer with a smaller deformation, although transition properties are not considered. Microscopically, the main component of the 0_2^+ is $\left(\nu[505]\frac{11}{2}\right)^2$ in this scenario. An important consequence of their argument is that this scenario leads to the non-existence of the $0_2^+ \otimes \nu[505]\frac{11}{2}$ band in the adjacent odd nuclei, ^{153}Gd and ^{155}Gd, because of the blocking effect. In an accompanying paper [17], the authors studied ^{155}Gd and concluded that the $0_2^+ \otimes \nu[521]\frac{3}{2}$ and the $\gamma \otimes \nu[505]\frac{11}{2}$ bands exist but the $0_2^+ \otimes \nu[505]\frac{11}{2}$ does not. Note here that $\gamma \otimes \nu[505]\frac{11}{2}$ is an unusually high-K band. That was also already observed in Ref. [59]; the spin assignments of these two works differ by one unit from each other.

Here we examine the results of RPA calculations on 1) the ground state of ^{154}Gd, 2) the $[521]\frac{3}{2}$ state of ^{155}Gd, and 3) the $[505]\frac{11}{2}$ state of ^{155}Gd, in order to see how the β vibrational calculation can account for the observed properties. Calculations for the odd-A cases are done on their ground states specified by blocking an appropriate quasiparticle state [60] obtained by the calculation for ^{154}Gd. The difference between ^{153}Gd and ^{155}Gd is specified by the chemical potential that gives the correct particle number. The interaction strengths $G_{\rm n}$, $G_{\rm p}$, and $\kappa_K^{(+)}$ are kept unchanged. The results are summarized in Table 2.

In the phonon wave function of the ^{154}Gd case, 1), large backward amplitudes $|\phi|$ stem from time-reversal pairs of prolate (low-Ω) orbitals, such as $|\phi| = 0.771$, 0.411, and 0.631 for $\left(\nu[660]\frac{1}{2}\right)^2$, $\left(\nu[521]\frac{3}{2}\right)^2$, and $\left(\nu[651]\frac{3}{2}\right)^2$, respectively. In contrast, the only large forward amplitude is that of $\left(\nu[505]\frac{11}{2}\right)^2$, $|\psi| = 0.995$. This proves that the main origin of the collectivity is different from the main forward component. In the case of the $[521]\frac{3}{2}$ of ^{155}Gd, 2), collectivity is reduced by blocking one of the prolate orbitals but the resulting β vibration is still collective enough. In the case of the $[505]\frac{11}{2}$ of ^{155}Gd, 3), the wave function is changed dramatically by losing the main forward component. Consequently, the $K = 0$ strength is pushed up to higher energies but still distinguishable from other non-collective states. We also confirmed that the γ vibration is almost not affected because there are no neutron quasiparticle states that constitute $K = 2$ pairs with $[505]\frac{11}{2}$. These results prove that the characteristics of the spectra of ^{154}Gd and ^{155}Gd can be accounted for in terms of the β vibration. However, it should be noted that the isomerism of 0_3^+ and the difference in the cross-sections of (p, t) and (t, p) transfers to 0_2^+ are outside the scope of the present calculation, which does not contain the quadrupole pairing.

(3) ^{156}*Gd.* Figure 5 compares $B(E2)$ of (a) β and (b) γ vibrations of heavier isotopes. This indicates that ^{156}Gd is located at the point where the β and γ vibrations have similar transition matrix elements

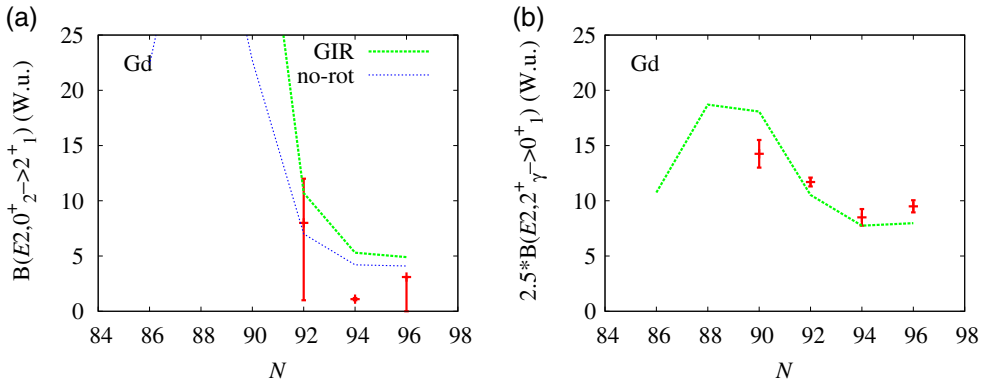

Fig. 5. (a) Low-$B(E2)$ part of Fig. 1(a). (b) $B\left(E2, 2^+_\gamma \to 0^+_1\right)$ multiplied by $\frac{5}{2}$ in order to compare the matrix elements with (a). The rotational effect does not appear in the latter. Data are taken from Ref. [18].

as well as excitation energies (Table 1). In this sense, ^{156}Gd can be regarded as a good example of Bohr–Mottelson's picture of deformed nuclei.

(4) ^{158}*Gd.* Figure 5(a) also indicates that the observed $B\left(E2, 0^+_2 \to 2^+_1\right)$ in ^{158}Gd looks evidently smaller than expected from the systematics. Actually this is one of the curious properties that have this nucleus extensively studied but have not yet been resolved. Since an early study [31], the 0^+_3 state at $E = 1452$ keV has been known to be more collective than the 0^+_2 state at $E = 1196$ keV. Although $\rho^2\left(E0, 0^+_2 \to 0^+_1\right)$ has not been reported up to now, $\rho^2\left(E0, 2^+_2 \to 2^+_1\right) = (0.72 \pm 0.21) \times 10^{-3}$ and $\rho^2\left(E0, 2^+_3 \to 2^+_1\right) = (25 \pm 4) \times 10^{-3}$ were reported in that work and reevaluated as $\leq 0.8 \times 10^{-3}$ and $(17 \pm 3) \times 10^{-3}$, respectively, in Ref. [9] for the rotational-band members. The quadrupole transition strengths were measured much later in Ref. [61] as $B\left(E2, 0^+_2 \to 2^+_1\right) = 1.1$ W.u. and $B\left(E2, 0^+_3 \to 2^+_1\right) = 2.1$ W.u.; see also Ref. [62]. In addition to the fact that the latter is larger, both of them are smaller than expected for ordinary β vibrations. Later, a large number of 0^+ states were reported [63]. Moreover, in Ref. [62], $B\left(E2, 0^+_n \to 2^+_1\right)$ was measured for a lot of states up to 0^+_{10}. This result proves that the $E2$ strengths are strongly fragmented and pushed up to higher energies; the largest one is $B\left(E2, 0^+_8 \to 2^+_1\right) = 7.7^{+1.5}_{-0.7}$ W.u. References [64,65] suggest a contribution of two-phonon octupole vibration to producing a large number of 0^+ states based on the geometrical collective model and the IBA model. In the projected shell model [66], the excited energies and the number of 0^+ states are accounted for by two- and four-quasiparticle states, but the associated $B(E2)$ are much smaller than observed. Lo Iudice et al. [29] and Gerçeklioglu [30] performed RPA calculations. The former includes the quadrupole pairing interaction. The resulting number of 0^+ states is less than observed in the RPA calculation, but quasiparticle–phonon couplings with octupole two-phonon states improve the result. The latter includes the spin–quadrupole interaction. The number of 0^+ states is reproduced without an octupole–octupole interaction. Both calculations, however, failed to account for the character of the 0^+_2 and 0^+_3 states. Our RPA result for the distribution of excited 0^+ states is presented in Fig. 6. The energy of the lowest excitation is fitted by adjusting the interaction strength $\kappa_0^{(+)}$. This figure shows that the overall distribution is reproduced quite well without an octupole–octupole interaction, but the obtained 0^+_3 is not collective. None of the higher states have $B(E2)$ strengths larger than 1 W.u.

One of the possible origins of quadrupole collectivity at high energies conjectured in Ref. [62] is the two-phonon γ vibration. The $K = 0$ two-phonon γ vibration is known only in ^{166}Er [67], although

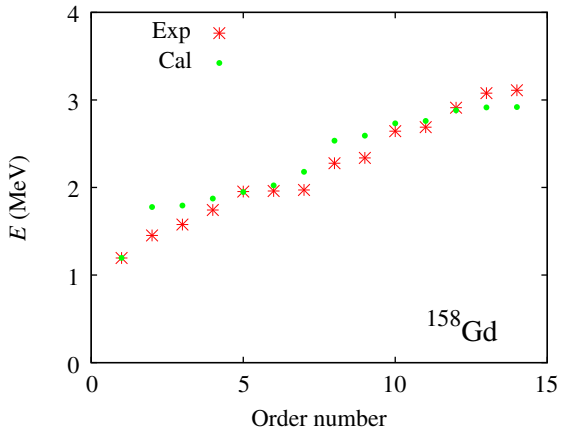

Fig. 6. Experimental and calculated distribution of excited 0^+ states in ^{158}Gd. Data are taken from Ref. [63].

the $K = 4$ ones are known more, as briefly reviewed in Ref. [68]. The quasiparticle–phonon coupling model calculation in Ref. [29] looks to include such a type of excitation, but the reported $B(E2)$ are much smaller.

(5) ^{160}*Gd.* Very recently, an upper limit of $B\left(E2, 0_2^+ \to 2_1^+\right)$ was reported [69]. The calculated value is slightly larger than the reported upper limit as shown in Fig. 5(a), but it is open whether there is a problem similar to ^{158}Gd.

4. Conclusions

The long-debated problem of the characterization of the 0_2^+ states in Gd isotopes has been revisited. The model adopted is a traditional mean field plus RPA. The doubly stretched quadrupole–quadrupole interaction is used. The rotational effect on the transition strengths are accounted for by that on the intrinsic matrix elements based on the generalized intensity relation. Calculations have been done paying attention to properties of rotational bands.

The most decisive property to characterize the 0_2^+ states is $B\left(E2, 0_2^+ \to 2_1^+\right)$. Its steep N dependence ranging two orders of magnitude is nicely reproduced. In particular, those in lighter isotopes, ^{152}Gd and ^{154}Gd, have been shown to be understandable as β-vibrational excitations on top of deformed ground states, as previously thought [2]. To this end, an implication of the strengths of $B(E2)$ and rotational properties for the former, and the relation to the spectra of the adjacent odd-A nucleus for the latter, have been investigated. Consequently, the present calculation supports the picture of Ref. [14]. The monopole transition strength, $\rho^2\left(E2, 0_2^+ \to 0_1^+\right)$, is also thought to be sensitive to the shape deformation/coexistence. The available data have been reproduced fairly well within the present model but data are still too scarce to utilize for discriminating different theoretical pictures.

Looking at relatively weak $B(E2)$ in heavier isotopes more closely, however, a disagreement remains in ^{158}Gd; a strong fragmentation of $B(E2)$ strengths to higher energies is not accounted for in the present model as well as in preceding works.

References

[1] A. Bohr and B. R. Mottelson, *Nuclear Structure* (Benjamin, New York, 1975), Vol. 2.
[2] P. E. Garrett, J. Phys. G **27**, R1 (2001).
[3] D. R. Bès and R. A. Broglia, Nucl. Phys. **80**, 289 (1966).

[4] D. G. Fleming et al., Phys. Rev. Lett. **27**, 1235 (1971).
[5] K. Heyde and J. L. Wood, Rev. Mod. Phys. **83**, 1467 (2011).
[6] Z. P. Li, T. Nikšić, and D. Vretenar, J. Phys. G **43**, 024005 (2016).
[7] P. Debenham et al., Nucl. Phys. A **195**, 385 (1972).
[8] J. O. Rasmussen, Nucl. Phys. **19**, 85 (1960).
[9] J. L. Wood, E. F. Zganjar, C. De Coster, and K. Heyde, Nucl. Phys. A **651**, 323 (1999).
[10] T. Yamada et al., Prog. Theor. Phys. **120**, 1139 (2008).
[11] T. Kibédi and R. H. Spear, At. Data Nucl. Data Tables **89**, 77 (2005).
[12] P. von Brentano et al., Phys. Rev. Lett. **93**, 152502 (2004).
[13] R. F. Casten et al., Phys. Rev. C **57**, R1553 (1998).
[14] D. G. Burke, Phys. Rev. C **66**, 024312 (2002).
[15] R. M. Clark et al., Phys. Rev. C **67**, 041302(R) (2003).
[16] J. F. Sharpey-Schafer et al., Eur. Phys. J. A **47**, 5 (2011).
[17] J. F. Sharpey-Schafer et al., Eur. Phys. J. A **47**, 6 (2011).
[18] *Table of Nuclides—Nuclear structure and decay data* (IAEA, Vienna, 2016). (Available at: https://www-nds.iaea.org/relnsd/vcharthtml/VChartHTML.html, date last accessed February 27, 2016).
[19] R. Bengtsson and I. Ragnarsson, Nucl. Phys.A **436**, 14 (1985).
[20] K. Kumar and M. Baranger, Nucl. Phys. A **122**, 273 (1968).
[21] J. B. Gupta, K. Kumar, and J. H. Hamilton, Phys. Rev. C **16**, 427 (1977).
[22] T. Kishimoto et al., Phys. Rev. Lett. **35**, 552 (1975).
[23] H. Sakamoto and T. Kishimoto, Nucl. Phys. A **501**, 205 (1989).
[24] Y. R. Shimizu and K. Matsuyanagi, Prog. Theor. Phys. **70**, 144 (1983).
[25] Y. R. Shimizu and T. Nakatsukasa, Nucl. Phys. A **611**, 22 (1996).
[26] T. Bengtsson, I. Ragnarsson, and S. Åberg, in Computational Nuclear Physics 1, eds. K. Langanke, J. Maruhn, and S. E. Koonin (Springer-Verlag, Berlin, Heidelberg, 1991), p. 51.
[27] D. R. Haenni and T. T. Sugihara, Phys. Rev. C **16**, 1129 (1977).
[28] W. Kulp et al., Phys. Rev. Lett. **91**, 102501 (2003).
[29] N. Lo Iudice, A. V. Sushkov, and N. Yu. Shirikova, Phys. Rev. C **70**, 064316 (2004).
[30] M. Gerçeklioglu, Eur. Phys. J. A **25**, 185 (2005).
[31] R. C. Greenwood et al., Nucl. Phys. A **304**, 327 (1978).
[32] J.- P. Delaroche et al., Phys. Rev. C **81**, 014303 (2010).
[33] S. Zerguine et al., Phys. Rev. Lett. **101**, 022502 (2008).
[34] A. A. Raduta et al., J. Phys. G **36**, 015114 (2009).
[35] N. Blasi et al., Phys. Rev. C **88**, 014318 (2013).
[36] N. Blasi et al., Phys. Rev. C **90**, 044317 (2014).
[37] S. Wang et al., Phys. Rev. C **72**, 024317 (2005).
[38] D. B. Campbell et al., Phys. Rev. C **75**, 064314 (2007).
[39] N. A. Matt et al., Phys. Rev. C **59**, 665 (1999).
[40] K. Kumar, Phys. Rev. Lett. **28**, 249 (1972).
[41] V. Werner et al., Phys. Rev. C **78**, 051303(R) (2008).
[42] S. W. Ødegård et al., Phys. Rev. Lett. **86**, 5866 (2001).
[43] G. Schönwaßer et al., Phys. Lett. B **552**, 9 (2003).
[44] H. Amro et al., Phys. Lett. B **553**, 197 (2003).
[45] M. Matsuzaki, Y. R. Shimizu, and K. Matsuyanagi, Phys. Rev. C **65**, 041303(R) (2002).
[46] D. Almehed, R. G. Nazmitdinov, and F. Dönau, Phys. Scr. T **125**, 139 (2006).
[47] Y. R. Shimizu, T. Shoji, and M. Matsuzaki, Phys. Rev. C **77**, 024319 (2008).
[48] T. Shoji and Y. R. Shimizu, Prog. Theor. Phys. **121**, 319 (2009).
[49] S. Frauendorf and F. Dönau, Phys. Rev. C **92**, 064306 (2015).
[50] I. Hamamoto, Phys. Rev. C **65**, 044305 (2002).
[51] R. F. Casten et al., Phys. Rev. C **67**, 064306 (2003).
[52] K. Tanabe and K. Sugawara-Tanabe, Phys. Rev. C **73**, 034305 (2006).
[53] D. A. Meyer et al., Phys. Rev. C **74**, 044309 (2006).
[54] M. A. M. Shahabuddin et al., Nucl. Phys. A **340**, 109 (1980).
[55] I. Ragnarsson and R. A. Broglia, Nucl. Phys. A **263**, 315 (1976).
[56] W. Kulp et al., Phys. Rev. C **69**, 064309 (2004).
[57] W. Kulp et al., Phys. Rev. C **77**, 061301(R) (2008).

[58] P. E. Garrett et al., Phys. Rev. Lett. **103**, 062501 (2009).
[59] T. Hayakawa et al., Nucl. Phys. A **657**, 3 (1999).
[60] Y. R. Shimizu and K. Matsuyanagi, Prog. Theor. Phys. **72**, 799 (1984).
[61] H. G. Börner et al., Phys. Rev. C **59**, 2432 (1999).
[62] S. R. Lesher et al., Phys. Rev. C **76**, 034318 (2007).
[63] S. R. Lesher et al., Phys. Rev. C **66**, 051305(R) (2002).
[64] N. V. Zamfir, J.-y. Zhang, and R. F. Casten, Phys. Rev. C **66**, 057303 (2002).
[65] K. Nomura, R. Rodríguez-Guzmán, and L. M. Robledo, Phys. Rev. C **92**, 014312 (2015).
[66] Y. Sun et al., Phys. Rev. C **68**, 061301(R) (2003).
[67] P. E. Garrett, Phys. Rev. Lett. **78**, 4525 (1997).
[68] M. Matsuzaki, Phys. Rev. C **83**, 054320 (2011).
[69] S. R. Lesher et al., Phys. Rev. C **91**, 054317 (2015).